Published in final edited form as:
*Toxicon*. 2010 ; 55(2-3): 325. doi:10.1016/j.toxicon.2009.08.007.

# The Algal Hepatoxoxin Okadaic Acid is a Substrate for Human Cytochromes CYP3A4 and CYP3A5

**Fujiang Guo**, **Tianying An**, and **Kathleen S. Rein***
Department of Chemistry and Biochemistry, Florida International University, Miami, FL 33199

## Abstract

The hepatotoxin okadaic acid (OA) was incubated with nine human recombinant cytochrome P450s (1A1, 1A2, 2C8, 2C9, 2C19, 2D6, 2E1, 3A4 and 3A5). Both CYP3A4 and CYP3A5 converted OA to a mixture of the same four metabolites, but incubation with CYP3A4 resulted in higher levels of conversion. Michaelis-Menten parameters, $K_m$ (73.4 $\mu$M) and $V_{max}$ (7.23 nmol of metabolites $nmol^{-1}$ $min^{-1}$) for CYP3A4 were calculated by analyzing double-reciprocal plots. LC-$MS^n$ analysis and chemical interconversion indicate that metabolites **2** and **3** are the 11*S*-hydroxy and 11*R*-hydroxy okadaic acid respectively, while metabolite **4** is 11-oxo okadaic acid. LC-$MS^n$ analysis of metabolite **1** shows a molecular ion which corresponds to an addition of 16 amu to OA, also suggesting hydroxylation, but the specific site has not been identified. The same four metabolites were produced upon incubation of okadaic acid with pooled human liver microsomes. This transformation could be completely inhibited with ketokonazole, and inhibitor of the CYP3A family of enzymes. The metabolites were determined to be only slightly less potent inhibitors of serine threonine protein phosphatase 2A (PP2A) when compared to OA. As PP2A is the principle molecular target for OA, these oxidative transformations may not effectively detoxify OA.

### Keywords

okadaic acid; diarrheic shellfish poisoning (DSP); cytochrome P450; metabolism; human liver microsome; protein phosphatase inhibitors

## 1. Introduction

Okadaic acid (OA, Fig. 1) and the related dinophysistoxins (DTX-1 and DTX-2) are produced by several dinoflagellates (marine phytoplankton) belonging to the genera *Prorocentrum* and *Dinophysis*. Consumption of OA-contaminated shellfish results in a syndrome known as diarrheic shellfish poisoning (DSP) which is characterized by severe gastrointestinal symptoms. DSP has been associated with the consumption of mussels, scallops or clams tainted with OA and its derivatives. DSP has worldwide distribution, however it appears to be most prevalent in Japan and Northern Europe (Luckas, et al., 2005;Yasumoto and Murata, 1993). The effects of long-term and chronic exposure to OA may be of greater concern, as it has been



*Corresponding author. Tel: 305-348-6682; Fax: 305-348-3772. reink@fiu.edu (K.S. Rein)



Conflict of interest
The authors declare that there are no conflicts of interest.

demonstrated to be a potent tumor promoter that differs from the phorbol ester class (Fujiki and Suganuma, 1993;Haystead, et al., 1989).

OA and DTX's are inhibitors of protein phosphatases PP1 and PP2A (Dounay and Forsyth, 2002). Inhibition of PP1/2A results in the hyperphosphorylation of many proteins in the cell and loss of regulation of cellular processes. OA can act both as a tumor promoter and inducer of apoptosis (Gehringer, 2004). A growing body of evidence suggests that OA exhibits genotoxic effects. Fessard demonstrated the formation of OA-DNA adducts in fibroblasts and keratinocytes (Fessard, et al., 1996). Tohda reported a positive Ames test in mammalian cells with OA (Tohda, et al., 1993). A statistically significant increase in micronucleous formation was observed in the haematocytes of the mussel *Perna perna*, upon exposure to OA (Carvalho Pinto-Silva, et al., 2003). Utilizing the cytokinesis-block micronucleous assay and fluorescence in situ hybridization (FISH), LeHegarat reported that OA had an aneugenic (chromosome loss) effect on CHO-K1 cells, but only after metabolic activation with a rat liver postmitochondrial S9 fraction (Le Hegarat, et al., 2003, 2004). This effect could be abolished by heat inactivation of the S9 fraction. The authors suggested that OA is metabolically activated to one or more genotoxic products.

A few studies on the distribution of OA in vertebrates have been reported. Two independent studies report the systemic distribution of tritiated OA to all organs examined after oral administration to mice. This included the heart, stomach, kidney, liver, skin, large and small intestines and bile (Matias, et al., 1996, 1999; Ito, et al., 2002). Highest concentrations within the first 24 hours were observed in the stomach, large and small intestines and bile. However, OA appeared to have the longest residence time in the liver, with detectable levels present up to two weeks after administration.

No studies on the metabolism of OA in vertebrates have been reported. However, Pfohl-Leszkowicz reported an induction of EROD activity 24 h and 48 h after injection of OA into the fish *Dicentrarchus labrax* (Pfohl-Leszkowicz, et al., 1998) which would be indicative of upregulation of the CYP1A family of enzymes. The metabolism of OA in shellfish has been described. Three OA metabolites, which were oxidized in the alcohol portion of the ester, were isolated from the diatom *Thalassiosira weissflogii*, and partially characterized (Windust, et al., 2000) although the specific site of oxidation was not identified. In bi-valves, OA, DTX-2 and DTX-1 are converted to complex mixtures of fatty acid esters, by acylation of the 7-hydroxyl group, collectively known as DTX-3 (Marr, et al., 1992; Vale and Sampayo, 1999; 2002; Torgersen, et al., 2008).

In this study, the effect of nine human cytochrome P450s (1A1, 1A2, 2C8, 2C9, 2C19, 2D6, 2E1, 3A4 and 3A5) on OA was examined. These enzymes were chosen because taken together, they represent on average 70% of the cytochrome P450s present in human liver and are the major enzymes involved in xenobiotic metabolism (Lewis, 2001). Among these nine cytochrome P450s, we observed that CYP3A4 and CYP3A5 converted OA into four oxidized metabolites.

## 2. Materials and methods

### 2.1 Chemicals and Biochemicals

Okadaic acid was isolated from cultures of *P. hoffmanianum* according to published methods (Hu, et al., 1992), prepared as the ammonium salt and compared by LC-MS to okadaic acid (> 99.7% purity) which was purchased from Calbiochem (San Diego, CA). Human recombinant cytochrome P450s were purchased from Codexis (Pasadena, CA). Pooled human liver microsomes were purchased from BD Biosciences (Woburn, MA). Protein phosphatase Type 2A was purchased from Upstate Biotechnology Inc. (Temecula, CA). HPLC-grade acetonitrile

was purchased from Fisher Chemicals (Fair Lawn, NJ). All other chemicals were purchased from Sigma-Aldrich (St. Louis, MO).

### 2.2 Confirmation of Enzyme Activity

All enzymes were determined to be active by incubating with positive controls according to previously described protocols; ethoxyresorufin deethylation for CYP 1A1 and 1A2 (Leclercq, et al., 1996); paclitaxel hydroxylation for CYP 2C8 (Cresteil, et al., 2002); harmin demethylation for CYP 2C9, 2D6 (Yu, et al., 2003); omeprazole hydroxylation for CYP 2C19 (Yamazaki, et al., 1997); chlorzoxazone hydroxylation for CYP 2E1 (Peter, et al., 1990); testosterone hydroxylation for CYP 3A4 and 3A5 (Krauser, et al., 2004).

### 2.3 Incubation of OA with P450s

Incubations were performed at 37 °C on a temperature-controlled shaker. The standard incubation (final volume 0.5 mL) contained 500 pmol of P450 enzyme, 50 $\mu$M of OA ammonium salt and reaction mix which contained an NADPH regeneration system provided by the manufacturer (Codexis, Pasadena, CA). The reaction mix/OA mixtures were vortexed and preincubated for 5 min at 37 °C prior to addition of enzyme. The reactions were monitored at 0, 30, 60 min. The reactions were quenched with an equal volume of cold methanol. The vial was vortexed and stored at - 20 °C for 20 min. The solution was centrifuged to remove precipitated protein and diluted to about 2.5 $\mu$M (OA concentration) with methanol. Proteins were precipitated a second time at - 20 °C for 20 min and centrifuged again. The samples were analyzed by LC-MS.

### 2.4 CYP3A4 Enzyme kinetics

From preliminary experiments it was established that the formation of metabolites from OA was linear for up to 15 min. Kinetic experiments were performed in 0.5 mL volume with OA ammonium salt concentrations ranging from 10-100 $\mu$M, 300 pmol of 3A4 enzyme and reaction mix. Reactions were monitored at 5, 7.5 and 10 min. The reactions were analyzed by LC-MS after workup described above.

### 2.5 Incubation of OA with pooled human liver microsomes

The standard incubation mixture (final volume of 0.5 mL) contained human liver microsomes (5.0 mg protein $mL^{-1}$), 0.1 M potassium phosphate buffer (pH = 7.4), an NADPH regenerating system consisting of 1.3 mM $NADP^+$, 3.3 mM glucose 6-phosphate and 0.4 U $mL^{-1}$ glucose 6-phosphate dehydrogenase, 3.3 mM $MgCl_2$ and 5 $\mu$M OA ammonium salt. Incubation was carried out at 37 °C for 30 min and terminated by adding an equal volume of cold methanol. The vial was vortexed and stored at - 20 °C for 20 min. The solution was centrifuged to remove precipitated protein. The sample was assayed by LC-MS.

### 2.6 LC-$MS^n$ Analyses

HPLC analysis was carried out on a Finnigan Surveyor series HPLC system (Thermo Fisher Scientific Inc., Waltham, MA). A 5 $\mu$m $C_{18}$, 250 mm × 4.6 mm Discovery column (Supelco, Bellefonte, PA) was used to separate metabolites. The chromatographic conditions were as follows: flow rate of 0.5 mL/min; solvent A, $CH_3CN$; solvent B, 2 mM $NH_4OAc$ buffer containing 0.05% formic acid; 0 - 25 min, 40% to 85% A (v/v); 25 - 30 min, 85% to 90% A (v/v); 30 - 35 min, hold at 90% A (v/v). MS analysis was performed on a Finnigan LCQ Deca XP MAX mass ion-trap spectrometer (Thermo Fisher Scientific Inc., Waltham, MA). Full-scan mass spectra were acquired in negative electrospray ionization (ESI) mode with collision energy of 35 eV, over the mass range *m/z* 500-1000. The sheath gas flow rate was 40 (arbitrary units) and the auxiliary gas was set at 10 (arbitrary units). The spray voltage was set at 3.5 kV and the capillary voltage was set at -45 V. The capillary temperature was set at 200 °C. A

setting of 35% normalized collision energy was applied to ions of all $MS^n$ experiments. Four metabolites were further purified by HPLC. The column effluent was split post column (1:4) with the smaller portion directed to the MS interface and the remainder of the effluent was collected. Fractions were dried in vacuuo and reanalyzed by LC-MS as described above. For enzyme kinetics experiments, total area normalization method was utilized to determine the relative contributions of OA and its metabolites. For protein phosphatase inhibition experiments with isolated metabolites, concentrations of metabolites were determined against a single point calibration curve generated by injecting 10 μL of a 6.2 μM solution (50 ng) of OA. The instrument's limit of detection (LOD, defined as S/N = 3) was 0.1 ng for OA.

### 2.7 Reduction of Metabolite 4

Ten $\mu$L of sodium borohydride ($NaBH_4$) in DMF (1 $\mu g\ \mu L^{-1}$) was added to a stirred mixture of metabolite 4 (~ 10 $\mu$g), cerium chloride heptahydrate (~ 1 mg) and methanol (1 mL). The mixture was stirred at room temperature for 30 min. Methanol was evaporated under a stream of $N_2$ and the residue was redissolved in 0.5 mL of $CH_2Cl_2$/MeOH (85:15, v/v). Residual salts were removed by rapid chromatography technique on a PrepSep Silica gel cartridge (Fisher Scientific, Fair Lawn, NJ). Elution was performed using 15 mL $CH_2Cl_2$/MeOH (85:15, v/v). Eluant was collected and evaporated to dryness under a stream of $N_2$ and the residue was reconstituted in 200 $\mu$L MeOH for LC-MS analysis.

### 2.8 Oxidation of Metabolite 2

To a solution of 20 $\mu$g of metabolite 2 in 200 $\mu$L of $CH_2Cl_2$ was added 20 $\mu$L of a suspension of activated $MnO_2$ in $CH_2Cl_2$ (4 mg $MnO_2$ per 1 mL $CH_2Cl_2$). The reaction mixture was stirred at room temperature for 30 min. $MnO_2$ was removed by 0.45 $\mu$ filter. The filtrate was evaporated under a stream of $N_2$ and redissolved in 200 $\mu$L of methanol for LC-MS analysis.

### 2.9 Protein Phosphatase 2A Inhibition Assay

The protein phosphatase inhibition assay was carried out in 96-well plates based on a method previously described (Simon and Vernoux, 1994; Tubaro, et al., 1996). Samples were allowed to incubate for 1 h at room temperature and read using a Bio-Tek Instruments Synergy 2 plate reader (Winooski, VT) scanning at 405 nm. A standard curve was prepared with pure OA, prepared exactly as the samples. Inhibitor concentrations giving 50% inhibition against the reference value was determined from dose-response curves of activity versus the log of concentration. $IC_{50}$ concentrations were calculated using the program Prism (v3, GraphPad Software).

## 3. Results and Discussion

### 3.1 Metabolism of okadaic acid by cytochrome P450s

Okadaic acid (OA) was incubated with nine recombinant human P450 enzymes (CYP1A1, 1A2, 2C8, 2C9, 2C19, 2D6, 2E1, 3A4 and 3A5). The reactions were monitored by LC-MS and the results indicated that CYP3A4 and CYP 3A5 metabolize OA, with CYP 3A4 resulting in higher turnover. The total ion current chromatogram obtained from the negative ion LC-MS analysis of the reaction mixture after incubation of OA with CYP 3A4 for 30 min is shown in Fig. 2B. Four new peaks eluting before OA ($t_R$ 23.75 min) in the LC-MS profile of the reaction mixture were observed, including two major peaks (metabolite 1, $t_R$ 13.15 min; metabolite 2, $t_R$ 17.92 min) and two minor peaks (metabolite 3, $t_R$ 19.23 min; metabolite 4, $t_R$ 20.65 min). These four metabolites were absent from the incubation mixture when quenched at 0 min (Fig. 2a) and increased with incubation time. Likewise, incubation of OA with CYP3A5 produced four peaks at the same retention times and having identical molecular ions as those of metabolites 1-4, suggesting that they are identical to metabolites produced by CYP3A4.

However, the overall conversion of OA was less in the CYP 3A5 reaction. After 6 hrs of incubation, the overall yield of all four metabolites was only 6.1% for the CYP 3A5 reaction while it was 31.3% for the CYP3A4 reaction. Within the limits of detection (0.1 ng OA) none of the seven other P450s metabolized OA when incubated under the same conditions, suggesting that those enzymes play no significant role in the metabolism of OA.

Preliminary experiments indicated that OA metabolism by CYP3A4 was linear up to 15 min (Fig. 3a). The Michaelis-Menten parameters, $K_m$ (73.4 $\mu$M) and $V_{max}$ (7.23 nmol of metabolites $nmol^{-1}$ $min^{-1}$) for the oxidation of OA by CYP3A4 were calculated by analyzing double-reciprocal plots (Fig. 3b) for incubations of OA with at concentrations ranging from 10 $\mu$M to 100 $\mu$M.

Okadaic acid (OA) was also incubated with pooled human liver microsomes (final protein concentration of 5 mg $mL^{-1}$). LC-MS analysis revealed that four metabolites, identical to those formed in CYP3A4 incubations, were produced (Fig. 2c), suggesting that OA can be metabolized by human liver. Within the limits of detection, this transformation was completely inhibited by the presence of 10 $\mu$M ketoconazole (Dilmaghanian, et al., 2004), a known CYP3A inhibitor. This result further suggested than in human liver, CYP3A is principally responsible for OA metabolism.

### 3.2 Characterization of metabolites

In the negative ESI full-scan mass spectrum, metabolites 1-3 produced the same molecular ion peaks $[M-H]^-$ at *m/z* 819, while metabolite 4 yielded a $[M-H]^-$ ion of *m/z* 817. A difference of 16 in the *m/z* ratios for the molecular ion peaks of metabolites 1-3 when compared to OA (*m/z* 803) is suggestive of a hydroxylation or epoxidation of the okadaic acid molecule.

$MS^n$ experiments were further employed to identify the structures of these metabolites. Some important fragments of OA and metabolites 1-4 are listed in Tables 1 and 2. In the $MS^2$ spectrum from deprotonated OA (*m/z* 803), two important intense negative ions at *m/z* 563 and 255 are typically observed (Fig. 4a). The former originates from the cleavage between C26 and C27, the latter results from RDA (retro Diels-Alder) cleavage in ring B (Fig. 1) (Torgersen, et al., 2008;Paz, et al., 2007;Gerssen, et al., 2008). From metabolites 1-3, negative parent ions $[M-H]^-$ at *m/z* 819 were selected to perform $MS^2$ measurements. Metabolite 1 displays major fragments *m/z* 563 and 255 (Fig. 4b) identical to OA in the $MS^2$ spectrum. On the other hand, a minor peak at *m/z* 321 in the $MS^2$ spectra of OA, possibly resulting from cleavage through rings D and E (Fig. 1), is replaced by *m/z* 337 in the $MS^2$ spectrum of metabolite 1. Noteworthy is the observation of a fragment of *m/z* 335 from DTX-1, an analog of OA which has a methyl group at C35 (Torgersen, et al., 2008). These observations support the conclusion that hydroxylation occurred in fragment C of metabolite 1.

In the $MS^2$ spectra of *m/z* 819 from metabolites 2 and 3 (Fig. 4c), *m/z* 563 and 255 are replaced by *m/z* 579 and 271, suggesting that a hydroxylation occurred in fragment A of metabolites 2 and 3. The $MS^2$ spectrum of *m/z* 817 from minor metabolite 4 is shown in Fig. 4d. Two major ions at *m/z* 577 and 269 were observed representing a difference of two protons when compared to fragment A from metabolites 2 and 3. This suggested the oxidation to a carbonyl in Fragment A of metabolite 4.

The relationship between metabolites 2 and 4 was established by chemical interconversions. Metabolite 2 was converted quantitatively to metabolite 4 by treatment with activated $MnO_2$ (Fatiadi, 1976). Furthermore, Luche reduction (Gemal and Luche, 1981) of metabolite 4 provided metabolite 2 exclusively. These chemical transformations established unequivocally that metabolite 2 is an allylic alcohol, metabolite 4 is an α,β-unsaturated carbonyl and that metabolites 2 and 4 resulted from oxidation of OA at the same carbon. Inspection of OA

identifies two allylic positions in fragment A: C-11 and C-43. The $MS^3$ spectrum of fragment A (*m/z* 269) from metabolite 4 (Fig. 5c and Table 2) yielded a fragment of *m/z* 241 (-28 amu) which was not present in OA or any of the other metabolites. This represents a loss of CO, indicating that metabolite 4 must have a keto group at C11.

The presence of fragment ions at *m/z* 201, 173, 167, 139, 111, 97 in the $MS^3$ spectra (from *m/z* 271) of metabolites 2 and 3 (Fig. 5a, 5b), and their identical fragmentation patterns (Fig. 6) indicate that these two metabolites must be stereoisomers. The fact that Luche reduction of metabolite 4 failed to produce metabolite 3 may be result of the conformational bias of the B ring. In solution, the B-ring of OA adopts a chair conformation with the alkyl groups equatorial (Matsumori, et al., 1995). The preferred axial attack of $NaBH_4$ on the C-11 ketone will yield the equatorial alcohol. Therefore, the configuration of the hydroxyl group at C-11 in metabolite 2 is assigned 11*S*. While metabolite 2 was oxidized completely to 4 by activated $MnO_2$, metabolite 3 was not oxidized under the same conditions. A stereochemical effect has been observed previously in the $MnO_2$ oxidation of 2-eno-pyranosides (Fraser-Reid, et al., 1971). Equatorial alcohols were readily oxidized whereas axial alcohols were resistant to oxidation. An axial orientation of the 11-hydroxyl group of metabolite 3 would require that metabolite 3 has the 11*R* configuration.

Two major metabolites 1 and 2 were analyzed for protein phosphatase inhibition. We were unable to isolate pure metabolite 3, however a mixture of 2 and 3 (54%: 46%) was also analyzed for protein phosphatase inhibition. The dose response curves for OA and it metabolites are shown in Fig. 7. As can be seen, OA strongly inhibited PP2A, with an $IC_{50}$ of 0.61 nM. The calculated $IC_{50}$ values for metabolites were only slightly higher than that of OA; 0.94 nM for metabolite 1; 1.34 nM for metabolite 2; 0.95 nM for a mixture of 2 and 3, respectively. The crystal structure of PP2A bound to OA, shows that the F and G-rings of OA are located in a hydrophobic binding pocket (Xing, et al., 2006). The site of oxidation for metabolite 1 is probably not deep in this pocket, as the $IC_{50}$ for metabolite 1 is similar to that of OA. Metabolites 2 and 3 have the hydroxyl group oriented toward and away from the enzyme, respectively and the relative $IC_{50}$s are consistent with this observation.

In conclusion, four human metabolites of OA have been prepared by incubation with CYP3A4 or CYP3A5. The metabolites were also formed upon incubation with pooled human liver microsomes. The cytochrome P450s that we examined are responsible for the majority of xenobiotic metabolism in human liver. However, it is important to note that other cytochrome P450s not tested could also be involved in the metabolism of OA. Because the small quantities of metabolites obtained preclude NMR studies, these metabolites have been tentatively characterized by a combination of $MS^n$ experiments and chemical transformations. The inhibition of PP2A by three of the four metabolites is only slightly lower than OA, suggesting that these transformations do not significantly detoxify OA. However, given that the $LD_{50}$ for OA with various liver cell lines ranges from 10-100 nM (depending on cell line) (Souid-Mensi, et al., 2008), it seems unlikely that these metabolites play a significant role in the toxicity of OA. Currently these reactions are being scaled up and metabolites will be evaluated for their toxicity. This work represents the preliminary steps toward a more thorough understanding of the metabolic fate, disposition and toxicity of OA and its metabolites.

## Acknowledgments

This work was supported by the National Institute of Environmental Health Sciences (NIEHS) Grant S11 ES11181, the NSF-NIEHS Oceans and Human Health Center Program (National Science Foundation grant 0432368 and NIEHS grant P50 ES12736-01).

## References


Carvalho Pinto-Silva CR, Ferreira JF, Costa RHR, Belli Filho P, Creppy EE, Matias WG. Micronucleus induction in mussels exposed to okadaic acid. Toxicon 2003;41(1):93–97. [PubMed: 12467666]

Cresteil T, Monsarrat B, Dubois J, Sonnier M, Alvinerie P, Gueritte F. Regioselective metabolism of taxoids by human CYP 3A4 and 2C8: structure-activity relationship. Drug Metab. Dispos 2002;30(4): 438–445. [PubMed: 11901098]

Dilmaghanian S, Gerber JG, Filler SG, Sanchez A, Gal J. Enantioselectivity of inhibition of cytochrome p450 3A4 (CYP3A4) by ketoconazole: testosterone and methadone as substrates. Chirality 2004;16 (2):79–85. [PubMed: 14712470]

Dounay AB, Forsyth CJ. Okadaic acid: the archetypal serine/threonine protein phosphatase inhibitor. Curr. Med. Chem 2002;9(22):1939–1980. [PubMed: 12369865]

Fatiadi AJ. Active manganese dioxide oxidation in organic chemistry - part I. Synthesis 1976;1976(2): 65–104.

Fessard V, Grosse Y, Pfohl-Leszkowicz A, Puiseux-Dao S. Okadaic acid treatment induces DNA adduct formation in BHK21 C13 fibroblasts and HESV keratinocytes. Mutat. Res 1996;361(23):133–141. [PubMed: 8980699]

Fraser-Reid B, Carthy BJ, Holder NL, Yunker M. An apparent stereochemical effect in $MnO_2$ oxidation of some allylic alcohols. Can. J. Chem 1971;49(18):3038–3045.

Fujiki H, Suganuma M. Tumor promotion by inhibitors of protein phosphatases 1 and 2A: the okadaic acid class of compounds. Adv. Cancer Res 1993;61(1):143–194. [PubMed: 8394044]

Gehringer MM. Microcystin-LR and okadaic acid-induced cellular effects: a dualistic response. FEBS Lett 2004;557(13):1–8. [PubMed: 14741332]

Gemal AL, Luche JL. Lanthanoids in organic synthesis. 6. The reduction of $\alpha$-enones by sodium borohydride in the presence of lanthanoid chlorides: synthetic and mechanistic aspects. J. Am. Chem. Soc 1981;103(18):5454–5459.

Gerssen A, Mulder P, Rhijn HV, Boer JD. Mass spectrometric analysis of the marine lipophilicbiotoxins pectenotoxin-2 and okadaic acid by four different types of mass spectrometers. J. Mass. Spectrom 2008;43(8):1140–1147. [PubMed: 18383308]

Haystead TAJ, Sim ATR, Carling D, Honnor RC, Tsukitani C, Cohen P, Hardie G. Effects of the tumour promoter okadaic acid on intracellular protein phosphorylation and metabolism. Nature 1989;337 (1):78–81. [PubMed: 2562908]

Hu T, Marr J, Defreitas ASW, Quilliam MA, Walter JA, Wright JLC. New diol esters isolated from cultures of the dinoflagellates *Prorocentrum lima* and *Prorocentrum concavum*. J. Nat. Prod 1992;55 (11):1631–1637.

Ito E, Yasumoto T, Takai A, Imanishi S, Harada K. Investigation of the distribution and excretion of okadaic acid in mice using immunostaining method. Toxicon 2002;40(2):159–165. [PubMed: 11689237]

Krauser JA, Voehler M, Tseng LH, Schefer AB, Godejohann M, Guengerich FP. Testosterone 1$\beta$-hydroxylation by human cytochrome P450 3A4. Eur. J. Biochem 2004;271(19):3962–3969. [PubMed: 15373842]

Le Hegarat L, Fessard V, Poul JM, Dragacci S, Sanders P. Marine toxin okadaic acid induces aneuploidy in CHO-K1 cells in presence of rat liver postmitochondrial fraction, revealed by cytokinesis-block micronucleus assay coupled to FISH. Environ. Toxicol 2004;19(2):123–128. [PubMed: 15037998]

Le Hegarat L, Puech L, Fessard V, Poul JM, Dragacci S. Aneugenic potential of okadaic acid revealed by the micronucleus assay combined with the FISH technique in CHO-K1 cells. Mutagenesis 2003;18 (3):293–298. [PubMed: 12714697]

Lewis, DFV. Guide to cytochromes P450 structure and function. CRC Press; Boca Raton, FL: 2001.

Leclercq I, Desager JP, Vandeplas C, Horsmans Y. Fast determination of low-level cytochrome P-450 1A1 activity by high-performance liquid chromatography with fluorescence or visible absorbance detection. J. Chromatogr. B 1996;681(2):227–232.

Luckas B, Dahlmann J, Erler K, Gerdts G, Wasmund N, Hummert C, Hansen PD. Overview of key phytoplankton toxin and their recent occurrence in the North and Baltic Seas. Environ. Toxicol 2005;20(1):1–17. [PubMed: 15712332]

Marr JC, Hu T, Pleasance S, Quilliam MA, Wright JLC. Detection of new 7-O-acyl derivatives of diarrhetic shellfish poisoning toxins by liquid chromatography-mass spectrometry. Toxicon 1992;30 (12):1621–1630. [PubMed: 1488771]

Matias WG, Creppy EE. Evidence for enterohepatic circulation of okadaic acid in mice. Toxic Subst. Mech 1996;15(4):405–414.

Matias WG, Traore A, Creppy EE. Variations in the distribution of okadaic acid in organs and biological fluids of mice related to diarrhoeic syndrome. Hum. Exp. Toxicol 1999;18(5):345–350. [PubMed: 10372758]

Matsumori N, Murata M, Tachibana K. Conformational analysis of natural products using long-range carbon-proton coupling constants: three dimensional structure of okadaic acid in solution. Tetrahedron 1995;51(45):12229–12238.

Paz B, Daranas AH, Cruz PG, Franco JM, Napolitano JG, Norte M, Fernandez JJ. Identification and characterization of DTX-5c and 7-hydroxymethyl-2-methylene-octa-4,7-dienyl okadaate from *Prorocentrum belizeanum* cultures by LC-MS. Toxicon 2007;50(4):470–478. [PubMed: 17540428]

Peter R, Bocker R, Beaune PH, Iwasaki M, Guengerich FP, Yang CS. Hydroxylation of chlorzoxazone as a specific probes for human liver cytochrome P-450IIE1. Chem. Res. Toxicol 1990;3(6):566–573. [PubMed: 2103328]

Pfohl-Leszkowicz, A.; Fessard, F.; Puiseux-Dao, S. Implication of okadaic acid on DNA adduct formation and EROD activity; Mycotoxins and Phycotoxins - Developments in chemistry, Toxicology and Food Safety, Proceedings of the 9th international IUPAC Symposium on Mycotoxin and Phycotoxin; Rome, Italy. 27-31 May 1996; 1998. p. 569-576.Alaken, Fort Collins, CO, USA

Simon JF, Vernoux JP. Highly sensitive assay of okadaic acid using protein phosphatase and paranitrophenyl phosphate. Natural Toxins 1994;2(5):293–301. [PubMed: 7866665]

Souid-Mensi G, Moukha S, Mobio TA, Maaroufi K, Creppy EE. The cytotoxicity and genotoxicity of okadaic acid are cell-line dependent. Toxicon 2008;51(8):1338–1344. [PubMed: 18538364]

Tohda H, Nagao M, Sugimura T, Oikawa A. Okadaic acid, a protein phosphatase inhibitor, induces sister-chromatid exchanges depending on the presence of bromodeoxyuridine. Mutat. Res 1993;289(2): 275–280. [PubMed: 7690896]

Torgersen T, Wilkins AL, Rundberget T, Miles CO. Characterization of fatty acid esters of okadacid acid and related toxins in blue mussels (*Mytilus edulis*) from Norway. Rapid Commun. Mass Spectrom 2008;22(8):1127–1136. [PubMed: 18335462]

Tubaro A, Florio C, Luxich E, Sosa S, Loggia RD, Yasumoto T. A protein phosphatase 2A inhibition assay for a fast and sensitive assessment of okadaic acid contamination in mussels. Toxicon 1996;34 (7):743–752. [PubMed: 8843575]

Vale P, Sampayo MMM. Esters of okadaic acid and dinophysis toxin-2 in Portuguese bivalves related to human poisonings. Toxicon 1999;37(8):1109–1121. [PubMed: 10400295]

Vale P, Sampayo MMM. Esterification of DSP toxins by Portuguese bivalves from the northwest coat determined by LC-MS - a widespread phenomenon. Toxicon 2002;40(1):33–42. [PubMed: 11602276]

Windust AJ, Hu T, Wright JLC, Quilliam MA, McLachlan JL. Oxidative metabolism by *Thalassiosira weissflogii* (Bacillariophyceae) of a diol-ester of okadaic acid, the diarrhetic shellfish poisoning. J. Phycol 2000;36(2):342–350.

Xing Y, Xu Y, Chen Y, Jeffrey PD, Chao Y, Lin Z, Li Z, Strack S, Stock JB, Shi Y. Structure of protein Phosphatase 2A core enzyme bound to tumor-inducing toxins. Cell 2006;12(2):341–353. [PubMed: 17055435]

Yamazaki H, Inoue K, Shaw PM, Checovich WJ, Guengrich FP, Shimada T. Different contributions or cytochrome P450 2C19 and 3A4 in the oxidation of omeprazole by human liver microsomes: effects of contents of these two forms in individual human samples. J. Pharmacol. Exp. Ther 1997;283(2): 434–442. [PubMed: 9353355]

Yasumoto T, Murata M. Marine Toxins. Chem. Rev 1993;93(5):1897–1909.

Yu AM, Idle JR, Krausz KW, Kupfer A, Gonzalez FJ. Contribution of individual cytochrome P450 isozymes to the O-demethylation of the psychotropic $\beta$-carboline alkaloids harmaline and harmin. J. Pharmacol. Exp. Ther 2003;305(1):315–322. [PubMed: 12649384]

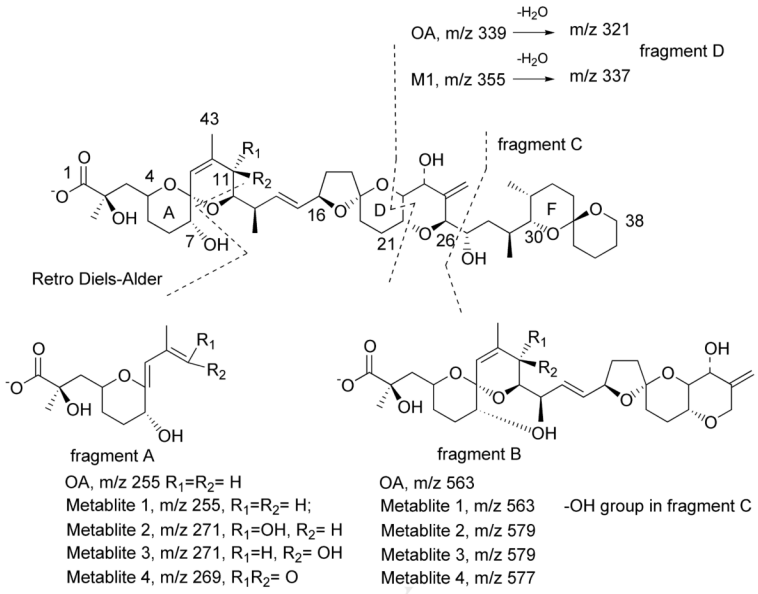


**Figure 1.**
Structure of OA and metabolites and proposed fragmentation pathways.

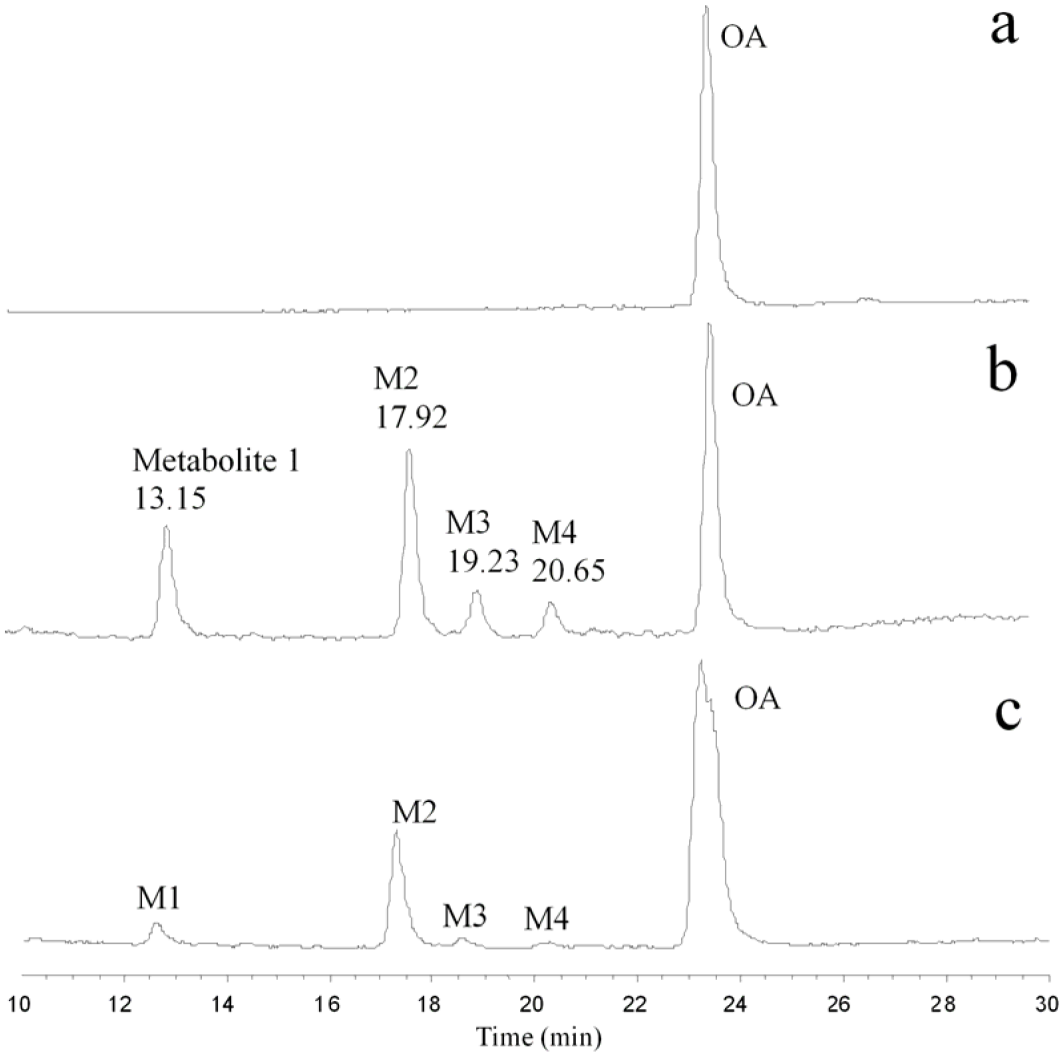


**Figure 2.**
Total ion chromatogram (TIC) of metabolic products of OA incubated with CYP3A4. (a) 0 h (b) 30 min. (c) Total ion chromatogram (TIC) of metabolic products of OA incubated with HLM. The mass range was from *m/z* 800 - 850.

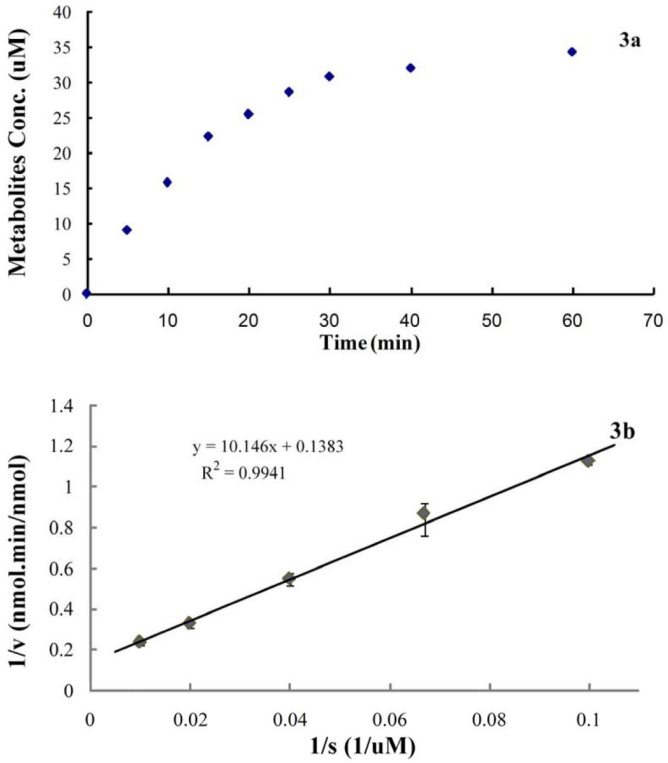


**Figure 3.**
(a) Metabolic profile of 50 μM OA incubated with 500 pmol CYP3A4 in 0.5 ml final volume.
(b) Double-reciprocal plot (1/V vs 1/S)

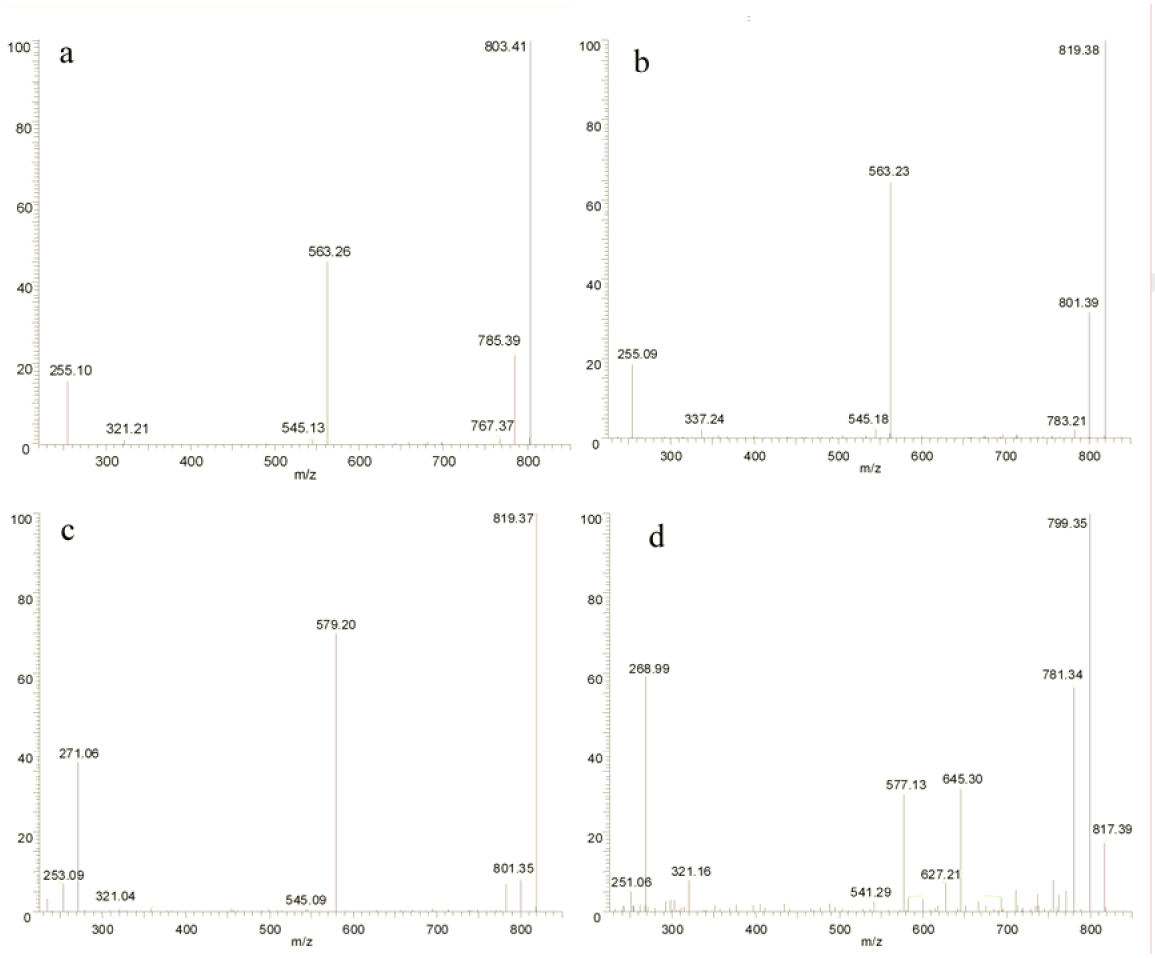


**Figure 4.**
Typical negative ESI MS/MS spectra of OA (a), metabolite 1 (b), 3 (c) and 4 (d).

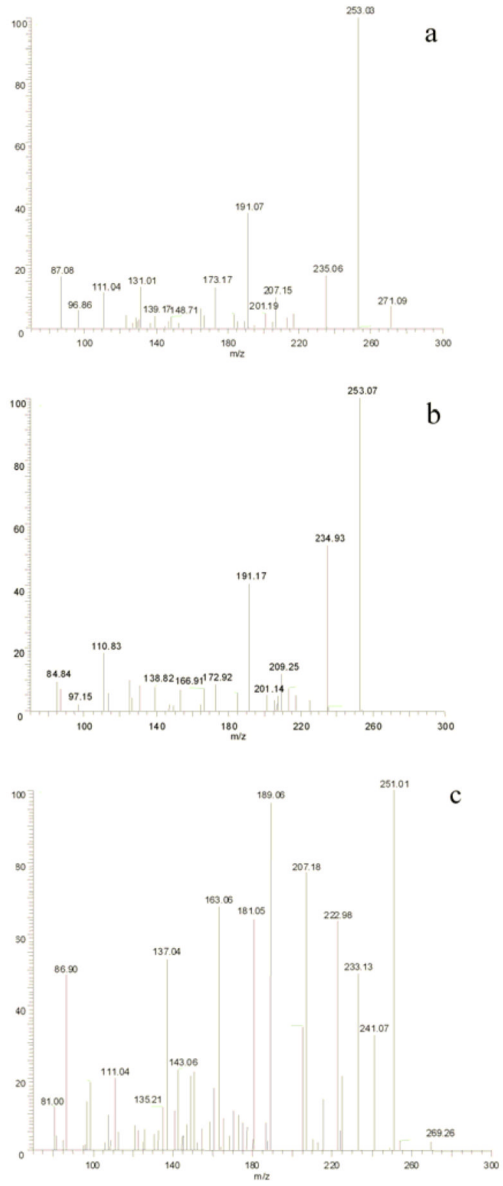


**Figure 5.**
$MS^3$ spectra of fragment A from metabolite 2 (a), 3 (b) and 4 (c) in negative ESI mode.

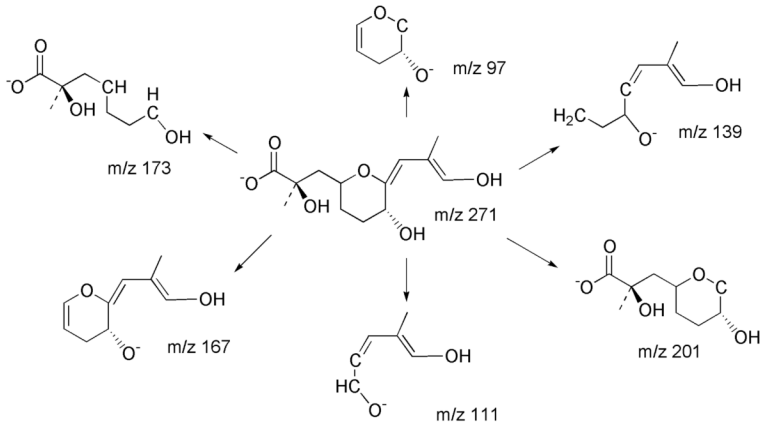


**Figure 6.**
Proposed $MS^3$ fragmentation pathways of *m/z* 271 from metabolites 2 and 3 in negative ESI mode.

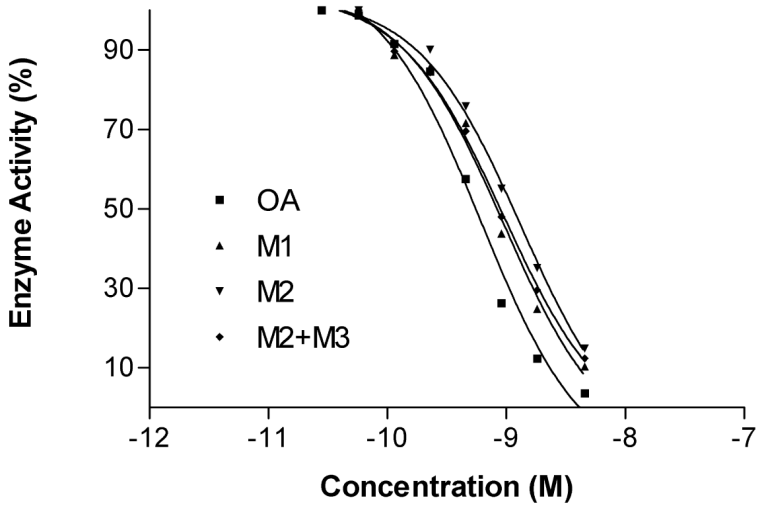


**Figure 7.**
The dose-response inhibitory activity of OA and its metabolites on PP2A .

**Table 1**

**Some important *m/z* values for fragment ions of deprotonated OA and metabolites 1-4 in negative ESI mode**

| | OA | 1 | 2 | 3 | 4 |
|---|---|---|---|---|---|
| $[M-H]^-$ | 803 | 819 | 819 | 819 | 817 |
| - $H_2O$ | 785 | 801 | 801 | 801 | 799 |
| - $H_2O$ | 767 | 783 | 783 | 783 | 781 |
| Frag B | 563 | 563 | 579 | 579 | 577 |
| - $H_2O$ | 545 | 545 | | | |
| Frag A | 255 | 255 | 271 | 271 | 269 |
| - $H_2O$ | | | 253 | 253 | 251 |
| Frag D | 321 | 337 | 321 | 321 | 321 |

**Table 2**

**Some important *m/z* values for $MS^3$ fragment ions from fragment A of OA and metabolites 1-4 in negative ESI mode**

| | OA | 1 | 2 | 3 | | 4 |
|---|---|---|---|---|---|---|
| Frag A | 255 | 255 | 271 | 271 | 269 | 241 (- CO) |
| - $H_2O$ | 237 | 237 | 253 | 253 | 251 | 223 |
| - $H_2O$ | 219 | 219 | 235 | 235 | 233 | 205 |
| - $CO_2$ | 175 | 175 | 191 | 191 | 189 | |